

Feasible Wrench Set Computation for Legged Robots

Ander Vallinas Prieto, Arvid Q.L. Keemink, Edwin H.F. van Asseldonk and Herman van der Kooij

Abstract—During locomotion, legged robots interact with the ground by sequentially establishing and breaking contact. The interaction wrenches that arise from contact are used to steer the robot’s Center of Mass (CoM) and reject perturbations that make the system deviate from the desired trajectory and often make them fall. The feasibility of a given control target (desired CoM wrench or acceleration) is conditioned by the contact point distribution, ground friction, and actuation limits. In this work, we develop an algorithm to compute the set of feasible wrenches that a legged robot can exert on its CoM through contact. The presented method can be used with any amount of non-coplanar contacts and takes into account actuation limits and limitations based on an inelastic contact model with Coulomb friction. This is exemplified with a planar biped model standing with the feet at different heights. Exploiting assumptions from the contact model, we explain how to compute the set of wrenches that are feasible on the CoM when the contacts remain in position as well as the ones that are feasible when some of the contacts are broken. Therefore, this algorithm can be used to assess whether a switch in contact configuration is feasible while achieving a given control task. Furthermore, the method can be used to identify the directions in which the system is not actuated (i.e. a wrench cannot be exerted in those directions). We show how having a joint be actuated or passive can change the non-actuated wrench directions of a robot at a given pose using a spatial model of a lower-extremity exoskeleton. Therefore, this algorithm is also a useful tool for the design phase of the system. This work presents a useful tool for the control and design of legged systems that extends on the current state of the art.

I. INTRODUCTION

Preventing dynamic instability during the locomotion of legged robots is of utmost importance. Dynamic instability can cause loss of balance and make the robot fall. Several works have developed stable walking trajectory generators using the concepts of Zero-Moment Point (ZMP) [1], extrapolated Center of Mass (CoM) [2], and its extensions (Instantaneous Capture Point [3] and Divergent Component of Motion [4]). The work of Dai et al. [5] used the Contact Wrench Cone (CWC) [6], a generalization of the ZMP criterion to multi-contact on uneven terrain, in order to improve the robustness of walking trajectories in humanoids. They improve the robustness of locomotion by generating trajectories that maximize the magnitude of perturbations that can be rejected.

However, most of the path planners that use the aforementioned concepts/approaches do not consider whether the wrench that needs to be applied on the CoM to follow the generated reference is feasible by the robot. Actuation limits

may significantly reduce the feasible wrenches and render some motion infeasible. Some notable works that explore how the actuation limits influence the feasible wrench or CoM manipulability are the work by Gu et al. [7] and the work by Orsolino et al. [8]. Both papers introduce different approaches to compute the set of feasible centroidal wrenches/accelerations that incorporate contact and actuation constraints.

Gu et al. introduce the Feasible CoM Dynamic Manipulability [7], which is an ellipsoidal approximation of the set of linear accelerations that a system can apply on its CoM through contact. Their work focuses only on the translation components of the CoM dynamics and takes into account static friction, actuation, and ZMP limits. The ZMP constraint is only applicable on flat terrain and restricts the usability of this analysis to such scenarios. Furthermore, their method is developed for a single foot contact.

Orsolino et al. [8] introduce the Actuation Wrench Polytope¹ (AWP), whose intersection with the CWC yields a new polytope named the Feasible Wrench Polytope (FWP). This polytope is claimed to contain all wrenches that a legged robot can exert on its CoM through contact, and thus, complies with actuation limits and a given contact model. This approach is more complete than the one presented in [7] because by using the CWC the whole body angular dynamics described at the CoM are also taken into account and the algorithm can be applied to any kind of terrain or multi-contact configuration.

Nevertheless, to reduce computation time, the method from [8] decouples the dynamics of the floating base² and each branch of the legged system. Furthermore, this method takes the actuation input and generalized accelerations of the system as inputs to compute the contact forces at each leg. However, ground reaction forces are *reactive* so the contact forces and generalized acceleration are fully determined by the system state and actuation input. Thus, for a given actuation input there is a corresponding contact force and the resulting generalized acceleration. This is, unfortunately, not the case when the algorithm from [8] is used, because with the same actuation input and different input accelerations, the resulting contact force is different. Therefore, decoupling floating base dynamics and providing accelerations as input

¹A polytope is an n -dimensional geometric object with flat faces. In this work, we only consider bounded convex polytopes, used to represent a bounded subset of n -dimensional space.

²Robots that do not have a base link that is fixed, are free to move through space. This freedom of motion is regarded as a 6 degree of freedom ‘joint’ (3 rotations and 3 translations) that has zero impedance, is non-actuated, and connects the world with a chosen link of the robot, which is called the floating base of the system.

The authors are with the Department of Biomechanical Engineering, University of Twente, Enschede, The Netherlands. This work is part of the research program Wearable Robotics, project number P16-05, (partly) financed by the Dutch Research Council (NWO).

introduce physical inconsistencies in their method, and their FWP is, therefore, not the polytope of all the feasible wrenches a robot can exert on its CoM through contact. We refer the reader to Appendix I for a mathematical description of their method and a proof of the physical inconsistencies it generates.

In this paper, we present a method to compute the set of feasible wrenches that a robot can exert on its CoM through actuation, which is dependent on pose and contact scenario. The resulting set is a physically correct FWP that does not decouple system dynamics nor require generalized accelerations as an input, which solves the limitations from [8]. This is achieved by using the knowledge of the contact model to constrain the generalized accelerations in such a way that, as dependent variables, they can be substituted in the system of equations and an actuation-to-force relationship is found.

The main contribution of this paper is the use of the contact model knowledge to build an algorithm that computes the set of feasible wrenches of a system at any given pose. The polytope obtained is the FWP of a robot that maintains the contact configuration. The second contribution of the paper is the extension of the algorithm to compute the set of feasible wrenches that results from opening some contacts. Push-off motions or complete foot detachment are two examples in which this extension is relevant.

The paper is structured as follows: Sec. II presents the proposed algorithm to compute a physically correct FWP. Sec. III shows two examples in which the method is applied: in Sec. III-A the algorithm is applied to a planar model of a biped in uneven contact configuration and in Sec. III-B the algorithm is used to compute the FWP of a spatial model of an under-actuated lower-body exoskeleton. Sec. IV discusses the attained results and Sec. V concludes the work.

II. METHOD

In this section, we present an algorithm that computes the contact forces for a given actuation input u and the system state, including the knowledge of contact locations.

A. Legged system model

The standard format of the Equations of Motion (EoM) of an articulate system is:

$$M(q)\dot{v} + h(q, v) = S_a u + \tau_e \quad (1)$$

where q is the vector of configuration variables and v is the vector of velocity variables³. $M(q)$ is the configuration-dependent mass-matrix and $h(q, v)$ is the vector of generalized forces due to gravity and velocity effects. The vector u consists of the actuation input (joint torques) and the selector matrix S_a maps the input into generalized forces. External generalized forces acting on the system are represented by τ_e . The only external forces considered in this work are contact reaction forces.

³The size of q is bigger than the size of v if a quaternion or $SO(3)$ element is used to represent the orientation of the floating base. In such a case $\dot{q} \neq v$.

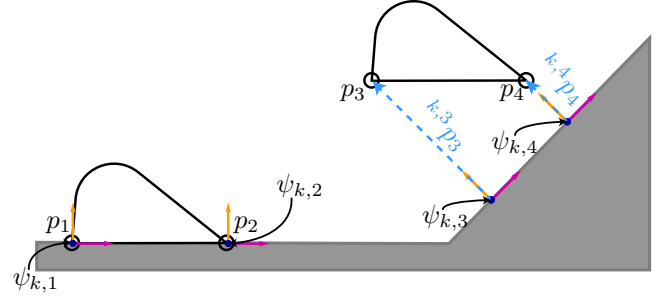


Fig. 1. Depiction of contact frames for a planar system with two feet. The dark blue dots represent the origin of each contact frame $\psi_{k,i}$, the normal direction is depicted in orange and the tangential direction in magenta. The first foot, with contact points p_1 and p_2 , rests over an un-inclined environment so the origins of $\psi_{k,1}$ and $\psi_{k,2}$ coincide with p_1 and p_2 respectively. The second foot, with contact points p_3 and p_4 , is not in contact with the environment so the origin of $\psi_{k,3}$ and $\psi_{k,4}$ do not coincide with the points ($\|^{k,3}p_3\|_2, \|^{k,4}p_4\|_2 \neq 0$) but are their projections on the environment.

External forces can be modeled as forces f_i acting on a body-fixed point of the system p_i . Contact forces arise when any p_i is in contact with the environment. For simplicity, it is common to pre-define contact locations (end-effectors, feet edges, fingertips,...) and assess whether the contact is active. We refer to contacts as active when the distance from the predefined contact point and the environment is zero. Each active contact force contributes to the generalized forces in the following manner:

$$\tau_e = \sum_{i=1}^{n_k} J_i^T(q) {}^{k,i}f_i \quad (2)$$

where k stands for contact, n_k is the number of active contacts and $J_i(q)$ is the Jacobian of contact point p_i in frame⁴ $\psi_{k,i}$:

$$J_i(q) = \frac{\partial ({}^{k,i}p_i(q))}{\partial q}.$$

The coordinate frames used in this work are the inertial frame ψ_0 , centroidal frame ψ_c , which shares orientation with ψ_0 but has the origin at the CoM of the system (x_c), and contact frames $\psi_{k,i}$, with the origin at a point on the environment closest to p_i (or the foot as a whole) and with the axes aligned with the tangential and normal directions with respect to the environment (see Fig. 1).

For simplicity (2) is rewritten in matrix form:

$$\tau_e = J^T(q)f = [J_1^T(q) \ J_2^T(q) \ \cdots \ J_{n_k}^T(q)] \begin{bmatrix} {}^{k,1}f_1 \\ {}^{k,2}f_2 \\ \vdots \\ {}^{k,n_k}f_{n_k} \end{bmatrix} \quad (3)$$

The total contact Jacobian $J(q)$ is constructed by stacking all the Jacobians of active contact points $J_i(q)$ and f is a stack of all active contact force vectors. For brevity, we will drop

⁴In this work, the coordinate frame $*$ is written as ψ_* . If a point, vector or screw is represented in ψ_* , this is denoted by the left superscript $*\cdot$.

the dependency of the aforementioned matrices and vectors on q and v .

Looking at (1) we see that given some state q, v and actuation input u we can solve for generalized accelerations \ddot{v} once the external forces are known. As contact forces are *reaction* forces, they are dependent variables as well. However, just with (1) the system of equations is underdetermined:

$$\begin{bmatrix} M & -J^T \end{bmatrix} \begin{bmatrix} \ddot{v} \\ f \end{bmatrix} = S_a u - h$$

Thus, a contact model is needed.

B. Contact model

In this work contact is modeled as purely inelastic in the same fashion of [9]. This contact model follows Signorini's conditions:

$${}^k p_N, {}^k f_N \geq 0, {}^k f_N {}^k p_N = 0 \quad (4)$$

where \square_N represents the normal direction in the contact frame. Notice that we have dropped the contact point index i and we use contact frame ψ_k because the contact model applies to all contact points.

We can re-write Signorini's conditions to velocity and acceleration constraints when the contact is active:

$${}^k \dot{p}_N, {}^k \ddot{p}_N, {}^k f_N \geq 0, {}^k f_N {}^k \dot{p}_N, {}^k f_N {}^k \ddot{p}_N = 0 \mid {}^k p_N = 0 \quad (5)$$

We will also consider Coulomb's friction model, which constrains tangential forces:

$$\|{}^k f_T\|_2 \leq \mu {}^k f_N \quad (6)$$

where μ is the static friction coefficient, and \square_T is used to denote the tangential direction in the contact frame.

To completely constrain contact forces we will adhere to the maximum dissipation principle, which states that contact forces minimize active contact velocity [9].

C. FWP computation

For each active contact point there are three possible scenarios [9]:

- 1) *Opening Contact*: When ${}^k \dot{p}_N > 0$ (or ${}^k \dot{p}_N = 0$ and ${}^k \ddot{p}_N > 0$), the contact is *opening*, in which case the contact becomes inactive and there is no reaction force: $\|{}^k f\|_2 = 0$
- 2) *Stick Contact*: The contact *cannot* penetrate the environment. If ${}^k \dot{p}_N \not> 0$, the speed in the normal direction must be zero. Furthermore, as the contact is not opening: ${}^k \dot{p}_N = 0, {}^k \ddot{p}_N = 0$. According to the maximum dissipation principle $\|{}^k \dot{p}\|_2$ must be minimal and, as long as (6) holds, the global minimum is zero. If the contact is completely static to start with ($\|{}^k \dot{p}\|_2 = 0$), the contact forces must ensure $\|{}^k \dot{p}\|_2 = 0$ and maintain the contact point in place. These forces that maintain the contact point in place will be called *stick* solutions.
- 3) *Slipping contact*: When the contact is not opening and the stick solution violates the friction cone constraint, the contact will *slip* ($\|{}^k \dot{p}_T\|_2 \neq 0$).

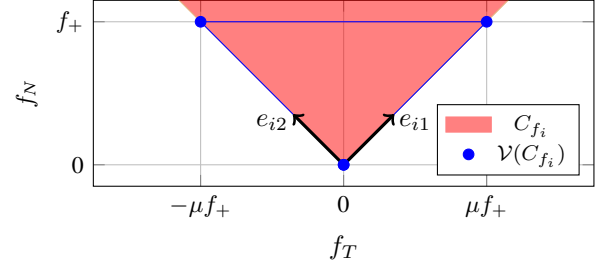


Fig. 2. Depiction of a single friction cone C_{f_i} on the plane. Any conical combination of e_{i1} and e_{i2} belongs to C_{f_i} , while a convex combination of $\mathcal{V}(C_{f_i})$ is a member of the bounded C_{f_i} .

If we focus on controlled legged locomotion, it is desirable to know the wrenches that can be applied on the CoM by:

- not changing the contact configuration. These wrenches are the stick solutions.
- taking a step or producing a push-off motion, which consists in opening some active contacts while the rest stick. These wrenches are the opening solutions.

Pure opening solutions (all active contacts open) correspond to jumping, in which no contact force can be applied. Slipping solutions are the result of infeasible stick solutions, and thus appear when the stick solutions intersect with the CWC. Slipping strategies could potentially be used for CoM control but are not considered in this work.

We briefly describe the construction of the CWC and next focus on the AWP computation. We will first find stick wrenches and then focus on the opening+stick wrenches.

1) *CWC construction*: The CWC is a convex cone that captures the friction and unilaterality constraints on the contact forces of all active contact points at once. This is achieved by the Minkowski summation [10] (denoted by the \oplus operator) of the friction cones that constrain the forces at each active contact point. The friction cones are non-linear in three-dimensional space but a linear approximation can be made by using j edge vectors e_{ij} that belong to the surface of the friction force cone of contact i (C_{f_i}). Any conical combination of these edges belongs to the friction cone. Furthermore, when an upper bound for the force in the normal direction is provided (f_+), the polyhedral cone is bounded and the set of forces belonging to C_{f_i} can be expressed in terms of its vertices (\mathcal{V} -description [11]).

To illustrate this we use the planar case (see Fig. 2), in which (6) becomes linear, and the cone can be described by two extreme rays. The \mathcal{V} -description of such a bounded cone in $\psi_{k,i}$ is given by:

$${}^{k,i} \mathcal{V}(C_{f_i}) = \begin{bmatrix} -\mu f_+ & 0 & \mu f_+ \\ f_+ & 0 & f_+ \end{bmatrix}, \quad (7)$$

where each column is a vertex and the first and second components correspond to the tangential and normal force.

The \mathcal{V} -description is convenient because the vertices of each friction cone can be expressed in a common frame in which each vertex has an associated moment and composes a wrench, generating individual wrench cones C_{w_i} . We express

these wrench vertices in ψ_c :

$${}^c\mathcal{V}(C_{w_i}) = \begin{bmatrix} ({}^0\tilde{p}_i - {}^0\tilde{x}_c) {}^cR_{k,i} {}^{k,i}\mathcal{V}(C_{f_i}) \\ {}^cR_{k,i} {}^{k,i}\mathcal{V}(C_{f_i}) \end{bmatrix}, \quad (8)$$

where ${}^cR_{k,i}$ is the rotation matrix from $\psi_{k,i}$ to ψ_c and $\tilde{\square}$ denotes the matrix-form of the vector cross product.

To conclude, the CWC is constructed by the Minkowski summation [10] of the wrench Cones C_{w_i} :

$$\text{CWC} = C_{w_1} \oplus \dots \oplus C_{w_{n_k}}. \quad (9)$$

2) *AWP: Stick solutions*: To find the *stick* solutions we constrain the acceleration of all active contacts to be zero. Contact point acceleration is expressed in terms of the generalized velocities, accelerations, and the contact Jacobian:

$${}^{k,i}\ddot{p}_i = J_i\dot{v} + \dot{J}_iv = 0. \quad (10)$$

These constraints are bilateral, which means that contact points can neither penetrate the contact surface nor *open*. The intersection of the stick solutions with the CWC will remove any contact wrench that is not consistent with the contact model either because the solution requires pulling on the contact (to prevent opening) or exceeds the maximum horizontal force due to friction [8].

The zero-acceleration constraint can only be used with established contacts ($\|{}^{k,i}\dot{p}_i\| = 0$). During impact events, the contact points have non-zero velocity, and therefore (10) cannot be applied to compute the contact forces. In this paper, we will only address established contacts.

Combining (10) with (1) the following system of equations is obtained:

$$\begin{bmatrix} M & J^T \\ J & 0 \end{bmatrix} \begin{bmatrix} \dot{v} \\ -f \end{bmatrix} = \begin{bmatrix} S_a u - h \\ -\dot{J}v \end{bmatrix}. \quad (11)$$

As \dot{v} can be written in terms of f and u , we find the following actuation-to-force relationship:

$$f = (JM^{-1}J^T)^+ (JM^{-1}(h - S_a u) - \dot{J}v). \quad (12)$$

where \square^+ represents the Moore-Penrose pseudo-inverse. Matrix $JM^{-1}J^T$ is square but might not be full rank. It is rank-deficient when J is rank-deficient. This happens whenever the system is in a singular pose (e.g. fully extended leg) and when a single rigid body (i.e. the foot) has multiple active contacts. In a singular pose, the system cannot move in one or more directions and the pseudo-inverse will bring the forces that excite motion in these directions to zero. Multiple active contacts within a single foot result in an underdetermined map from (foot) contact wrench to contact forces. However, the pseudo-inversion will minimize the forces while attaining the correct foot wrenches and, therefore, the correct wrench at the CoM. In both events, which are not mutually exclusive, the pseudo-inversion minimizes the norm of the resulting forces and the found wrench solution is physically correct. Furthermore, any infeasible wrench will be rejected when the AWP intersects with the

CWC. Thus, taking the pseudo-inverse to compute contact forces gives the correct FWP.

We have that u is bounded on each entry r :

$$u_r \in [u_r^-, u_r^+], \quad (13)$$

with $u_r^- < 0 < u_r^+$. Thus, the actuation space can be regarded as a convex polytope (U) whose half-plane (\mathcal{H} -)description [11] is given by:

$$\begin{bmatrix} \mathbb{I}_{n_a} \\ -\mathbb{I}_{n_a} \end{bmatrix} \begin{bmatrix} u_1 \\ \vdots \\ u_{n_a} \end{bmatrix} = A_a u \leq \begin{bmatrix} u_1^+ \\ \vdots \\ u_{n_a}^+ \\ -u_1^- \\ \vdots \\ -u_{n_a}^- \end{bmatrix} = b_a, \quad (14)$$

where \mathbb{I} is the identity matrix (of size equal to the subscript) and n_a equals the number of actuators.

The \mathcal{V} -description of U is given by all possible combinations of actuation limits and as such it is composed of 2^{n_a} points. Solving (12) for all members of $\mathcal{V}(U)$ gives the vertices of another convex polytope F_s , the set of all possible forces that would maintain the contacts in place given all possible actuation input. We can convert all force vertices to wrench vertices by this operation⁵ similar to (8):

$${}^cW = \begin{bmatrix} {}^0\tilde{p}_1 - {}^0\tilde{x}_c & \dots & {}^0\tilde{p}_{n_{ct}} - {}^0\tilde{x}_c \\ \mathbb{I}_3 & \dots & \mathbb{I}_3 \end{bmatrix} {}^0f, \quad (15)$$

where 0f is a member of F_s with all contact forces expressed in ψ_0 . The polytope of wrenches that arise from evaluating (15) with all ${}^0\mathcal{V}(F_s)$ will be called AWP_s . The intersection of the AWP_s with the complete CWC yields the FWP_s .

3) *AWP: Opening solutions*: In order to compute forces that are feasible when some of the active contacts *open*, the reasoning is the following:

- 1) The set of active points that we choose to *open* produce zero force ($\|f_o\|_2 = 0$), so we only need to solve for the forces of the active contacts that *stick* (f_s)
- 2) The set of active points that *stick* cannot accelerate ($\|\ddot{p}_s\|_2 = 0$) and the active contacts that open cannot penetrate the environment ($\ddot{p}_{oN} \geq 0$)

Thus, (11) is altered to constrain the motion of the *stick* contacts only, and account for the force only in those points:

$$\begin{bmatrix} M & J_s^T \\ J_s & 0 \end{bmatrix} \begin{bmatrix} \dot{v} \\ -f_s \end{bmatrix} = \begin{bmatrix} S_a u - h \\ -\dot{J}_s v \end{bmatrix}, \quad (16)$$

where J_s is the stack of contact jacobians corresponding to the active contacts that stick, and (12) changes to

$$f_s = (J_s M^{-1} J_s^T)^+ (J_s M^{-1}(h - S_a u) - \dot{J}_s v). \quad (17)$$

To prevent penetration of the contact surface by the *opening* points the following inequality must hold:

$$J_{oN}\dot{v} + \dot{J}_{oN}v \geq 0, \quad (18)$$

⁵In planar systems it reduces to two forces and the resulting moment.

where J_{oN} represents the normal component of the stack of contact jacobians corresponding to the active points that open.

To incorporate this inequality in our formulation, we express it in terms of u . The intersection of this constraint with U generates a new polytope U_o , which is a convex polytope of actuation inputs that do not violate the constraint in (18). The \mathcal{H} -description of U_o , namely $\mathcal{H}(U_o)$, is equal to $\mathcal{H}(U)$ with the added non-penetration constraint:

$$\begin{bmatrix} A_a \\ A_{np} \end{bmatrix} u \leq \begin{bmatrix} b_a \\ b_{np} \end{bmatrix}. \quad (19)$$

The non-penetration constraint in $\mathcal{H}(U_o)$ can be obtained by algebraic manipulation of (18), by substituting \dot{v} by the EoM (1) and then substituting f_s with (17). Isolating u yields the following inequality:

$$\begin{aligned} A_{np}u &\leq b_{np} \\ A_{np} &= -J_{oN}M^{-1}(\mathbb{I} - \Lambda_s J_s M^{-1})S_a \\ b_{np} &= \dot{J}_{oN}v - J_{oN}M^{-1}\left(h - \Lambda_s\left(\dot{J}_s v - J_s M^{-1}h\right)\right) \\ \Lambda_s &= J_s^T (J_s M^{-1} J_s^T)^+ \end{aligned} \quad (20)$$

Using a vertex enumeration algorithm we can find $\mathcal{V}(U_o)$. When we evaluate these vertices in (17) we obtain the set of forces that maintain the chosen active contacts in place while the other contacts *open*. Translating these forces to wrenches we get the AWP_o , which is another convex polytope. The intersection of a AWP_o with the corresponding CWC_o (built with the C_{f_i} of the points that stick) yields a FWP_o .

For a given contact configuration with n_k contact points there is one FWP_s and $2^{n_k} - 2$ FWP_o . The union of FWP_s and all non-empty FWP_o yields the FWP, which is the (non-convex) set of wrenches that the system can exert on its CoM through actuation.

All results shown in this work were attained using Matlab 2020a with a parallel pool of 6 workers to compute the AWP_s and AWP_o -s. All polytope intersections and double-description operations in this work were computed using [12].

III. EXAMPLES

A. FWP of a planar biped model

To illustrate the added value of our method we apply the algorithm to a planar model of an anthropomorphic biped climbing stairs. When a biped climbs stairs (as shown in Fig. 3), it confronts multi-contact situations (double support phase) on uneven terrain (the contacts are not at the same height), in which case the ZMP constraint cannot be used. The biped model consists of a torso and two legs with hip, knee, and ankle joints, and the segment length and inertial properties are computed for the standardized model by Winter [13] for a human that is 1.7 m tall and weighs 70 kg.

With a friction coefficient $\mu = 0.5$ and torque limits $u^\pm = \pm 100\text{Nm}$ for all joints (hips, knees, and ankles), the FWP_s of the biped model at the configuration shown in Fig. 3 and zero

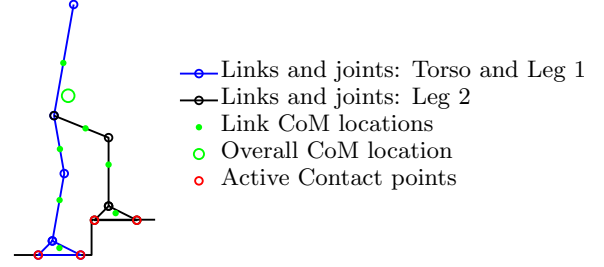


Fig. 3. Biped planar model with both feet in contact on uneven terrain.

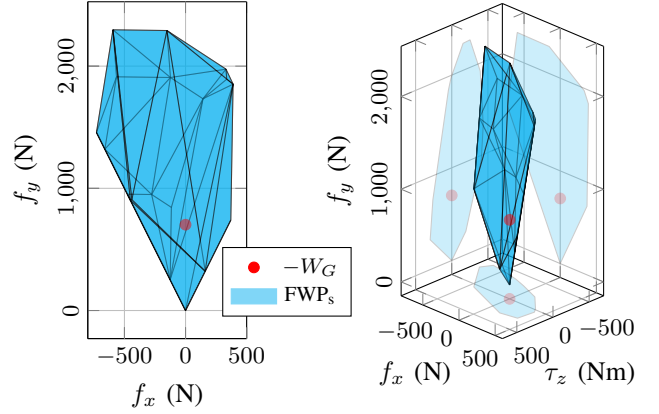


Fig. 4. FWP_s of the biped model in the configuration depicted in Fig. 3 and gravity compensation wrench ($-W_G$) with their projections in the principal back-planes. On the left panel the FWP_s is presented as the projection of the whole polytope in the linear force plane, similar to the results analyzed in [7]. On the right, the complete wrench space is shown, and the feasible moments around the CoM are also visible. All wrenches are expressed in ψc : x -axis corresponds to the horizontal direction, y -axis to the vertical and the z -axis is the direction out of the page (counter-clockwise rotation as positive).

joint velocity is presented in Fig. 4. On the left, the linear forces are shown. The friction cone constraint produces a sharp tip at zero force and follows the linear slope defined by μ , which is clearly depicted in this figure. On the right, the full FWP_s is shown. Looking at the complete polytope and its side projections one can see that also a moment may be applied around the CoM. In this case, as the polytope has non-zero volume, the system can exert the same force on the CoM with various resulting moments. This is because the force distribution can be modulated through all four contact points.

As presented in Sec.II, the FWP_s only contains the wrenches that are feasible when all the contacts stick. Fig. 5 shows the FWP_s superposed with FWP_o for two different contact opening situations. The first FWP_o , on the left, is the set of feasible wrenches if a push-off motion is started (the heel of the trailing leg detaches while the toe remains in contact). This polytope shows that a (slightly) greater positive moment can be applied on the CoM when the heel detaches than when the whole foot remains in place, while the feasible force in the positive horizontal direction is reduced. The second FWP_o (Figure 5, right panel) corresponds to a complete opening of the foot of the trailing leg. This FWP_o is completely contained in the FWP_s .

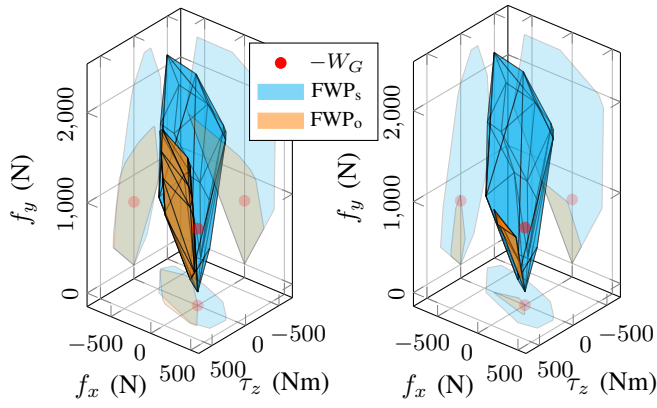


Fig. 5. Gravity compensation wrench ($-W_G$), FWP_s and two different FWP_o of the biped model in the configuration depicted in Fig. 3 with their projections in the principal back-planes. Left FWP_o : all points stick except the heel of the trailing leg. Right FWP_o : the foot of the trailing leg opens and the other foot sticks. All wrenches are expressed in ψ_c .

and the feasible wrenches decrease significantly in magnitude in all directions, although the forces and moments can be independently modulated to some extent.

The system is statically unstable in all of these opening contact scenarios because static gravity compensation is not feasible⁶. However, with the push-off opening contact configuration, the biped can compensate gravity while some added moment is applied around the CoM. Thus, the resulting linear acceleration can be zero but in such a case the whole-body angular momentum rate will not be zero.

In more challenging situations (e.g. standing on a single contact point) all feasible forces will have an associated moment that cannot be independently modulated. This is illustrated in Fig. 6, where we show the FWP_s already shown in Fig. 4 but add the FWP_o corresponding to a situation in which all the contact points from Fig. 3, except the toe of the trailing leg open. Therefore, any desired wrench outside of this (hyper-)plane (be it desired change in centroidal momentum or gravity/disturbance compensation) is not feasible. Only its projection onto the FWP_o is feasible and therefore the system will accelerate in the non-compensated direction.

B. FWP of a three-dimensional exoskeleton model: Comparison of passive and active DoF

In this section, we apply the method to a spatial model, where the centroidal wrench has 6 components (three moments and three forces). Due to the higher dimension of this space, the polytopes cannot be easily visualized and the results are more challenging to interpret. Nevertheless, the FWP is a useful tool to evaluate the design of an articulated system.

To exemplify this we use a rigid multi-body mathematical model of our Symbitron exoskeleton [14], which is a lower-body exoskeleton with 6 joints per leg: hip endo-exo rotation, hip abduction-adduction, hip, knee, and ankle flexion-extension, and ankle in-eversion. The hip endo-exo rotation is

⁶In the case of the push-off FWP_o is particularly clear that projections of the polytope are not sufficient to visualize the result, as the projections contain the projection of gravity compensation but the polytope does not.

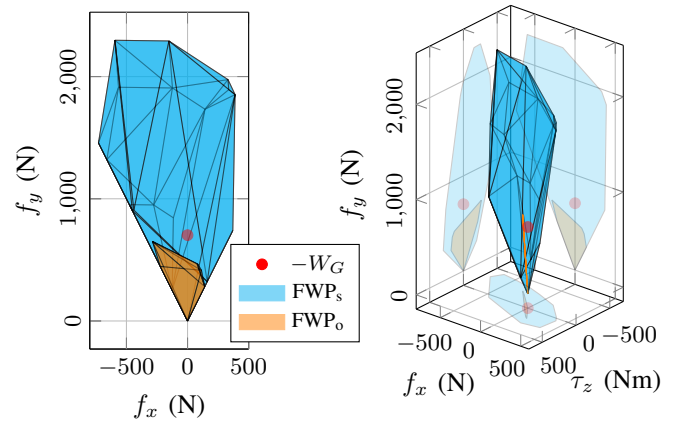


Fig. 6. Gravity compensation wrench ($-W_G$), FWP_s and a ‘weak’ FWP_o (standing on a single toe) of the biped model in the configuration depicted in Fig. 3 (with their projections in the principal back-planes) shown from two different perspectives. Left: Linear Force plane. Right: perpendicular to the ‘weak’ FWP_o , which is flat (edges emphasized with orange color). All wrenches are expressed in ψ_c .

spring-loaded and the ankle in-eversion is non-actuated. The non-actuated joints can be locked and we restrict this analysis to a model in which the hip endo-exo rotation is locked. Therefore, the exoskeleton model has a 6 DoF floating-base joint and 10 revolute joints, 2 of which are passive (achieved by setting the actuation limits u^\pm of passive joints to zero in (14)). We use the same μ and u^\pm (in the actuated joints) as Sec. III-A.

The FWP_s of the system in the configuration shown in Fig. 7a determines that the exoskeleton is in static equilibrium configuration as gravity compensation is feasible. However, the FWP_s is singular as it is contained in a (hyper-)plane, like the FWP_o shown in Fig. 6, instead of being full-dimensional. Thus, there is a wrench direction in which the system is not actuated. The singular (non-actuated) direction for this configuration is a pure moment around the axis shown by the blue vector in Fig. 7a. Any actuation input that maintains the contact configuration will elicit the same moment around this axis so the whole-body angular momentum rate of change in this direction is constant (in the absence of perturbations). As the system is in static equilibrium, the feasible moment around the singular axis is zero. A good example in which this is not the case was shown in Fig. 6, where, regardless of the actuation input, the resulting centroidal wrench will belong to the plane and the moment will be non-zero.

For comparison, we checked the FWP_s of the exoskeleton at the same configuration, now assuming that the ankle in-eversion was actuated, with the same actuator limits as the rest of the joints. The results show that the system would be non-actuated in the same direction. Therefore, the only way to excite the momenta in this direction (through internal forces) is by changing contact configuration.

The benefit of actuated over passive ankle in-eversion is clearer during single support. The FWP_s of the exoskeleton at the configuration in Fig. 7b is singular in the direction determined by the moment around the blue arrow and linear force along the green arrow when the ankle in-eversion is passive but it would be full dimensional, which means that

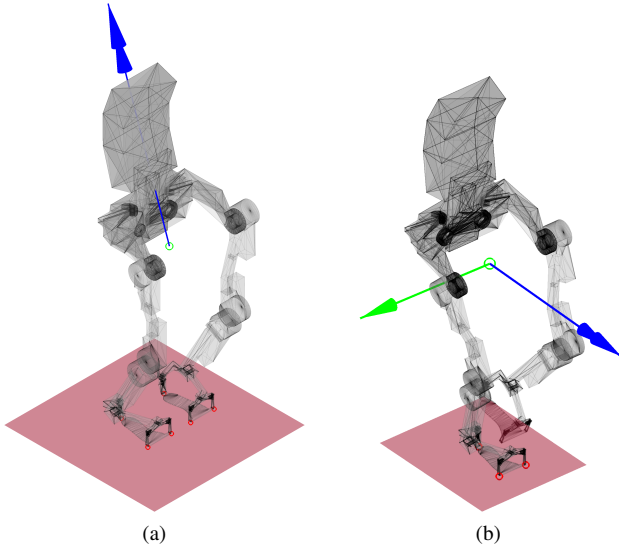


Fig. 7. Model of the Symbion exoskeleton in two different configurations and the corresponding singular wrench directions. The green marker represents the location of the CoM, the red markers show the active contact point locations. (a) Parallel feet double support stance with a little crouch. The blue (double headed) vector represents the non-actuated direction. A moment around this vector is not feasible with the depicted contact configuration. (b) Single support stance in static equilibrium. The blue (double headed) and green (single headed) vectors represent the six components of a unitary CoM wrench in the non-actuated direction. A moment around the blue arrow combined with a force along the green arrow is not feasible (where the moment/force proportion is given by the vector lengths) with the depicted contact configuration if the ankle in-eversion joint is passive.

all momenta would be independently actuated, if the ankle in-eversion were actuated.

IV. DISCUSSION

In this work, we developed an algorithm to compute the set of feasible wrenches that a legged robot can exert on its CoM through contact. The proposed method can be used at any contact configuration and takes into account actuation limits and a contact model to determine what wrenches are feasible.

The presented algorithm is an extended version of centroidal manipulability [7] that includes not only rotational dynamics but can also deal with multi-contact situations in uneven terrain like the one shown in Fig. 3.

The method also overcomes the physical inconsistencies from [8] by completely determining reaction forces and generalized accelerations from the system state and actuation input and, therefore, it yields the correct set of feasible wrenches. In [8] the FWP is used to maximize robustness in trajectory optimization with prescribed contact locations and instants and our algorithm can be used for the same purpose. The main drawback is that our algorithm is slow (the FWP_s in for Fig. 7a was computed in 10.077 s) and even if faster software was used for the computations, the number of operations that our algorithm requires is bigger compared to their approach because matrix sizes are bigger. Nevertheless, the advantage of using our algorithm to compute the FWP in trajectory optimization instead of theirs is that the robustness metric maximized in [8] (a relative

measure of the leftover wrench space) would be physically correct. Therefore, although the computation time will be longer if our algorithm is used for trajectory optimization, the trajectory will maximize a physically correct robustness metric.

Furthermore, besides showing the capabilities of the system at a given pose, the presented algorithm can also compute the feasible wrenches when some of the contact points open: the FWP_o-s. These computations can be used to assess whether a change in contact configuration is feasible while still attaining the desired rate of change in centroidal momentum so they can be useful to trigger contact changes and for trajectory planning. In Fig. 5 and 6 we see that none of the shown FWP_o contains the gravity compensation wrench. Thus, the switch to any of these three contact configurations will excite centroidal dynamics: any actuation that achieves the opening configuration will apply a moment around the CoM and/or make it accelerate. Although the system is not in a static equilibrium when these contacts open, it can still move, which may align with the desired control task.

The algorithm can also be used for comparison purposes and provide useful information on the actuated vs. non-actuated directions of the centroidal wrench. We have shown how some mechanical choices, like the use of passive joints, can have a big impact on the resulting FWP and this information can be used in the mechanical and mechatronic design of the system. Furthermore, prior knowledge of the non-actuated directions can assist in controller design. Any undesired acceleration in the non-actuated direction may result in a fall and is in turn a good indicator to take a step.

In this paper, for simplicity, the articulated systems that have been used as examples have flat rigid feet. Nevertheless, legged robots can have flexible feet, which are compliant and have a continuously varying contact surface. Any foot model (and joint impedance) can be easily included to analyze its effect. The addition of a toe-like joint, for example, is trivial and can be a first approximation of the time-varying contact surface.

The presented method has, however, one big limitation: the method cannot compute the effect of impacts (end effectors at contact distance with the environment and non-zero speed) on the feasible wrenches. This is particularly relevant during locomotion, where feet come in contact with the ground with non-zero velocity. In regular bipedal gait, the system is unstable in a dynamic sense during the latter part of the leg swing motion (the extrapolated CoM is outside of the BoS [2]). Heel strike has a twofold effect on stability:

- 1) The impact prevents ground penetration so, according to the contact model we consider in this work, it generates a kinematically-ideal instantaneous change in velocity. The magnitude of the impulse that achieves this change can be computed, but, as the event is discrete, the force is infinite.
- 2) Impact increases the BoS of the system, which renders the system dynamically stable again.

This method can only show the difference due to the increase in the BoS but cannot predict the change in foot velocity nor the forces arising from the impact.

V. CONCLUSION

In this work, we present a complete algorithm to compute all the Feasible Wrenches on the CoM of a floating-base articulated system (legged robots in particular) given its state, the actuation limits and the assumption of inelastic contact. This method extends on the methods presented in literature and can be used to analyze the strengths and weaknesses of floating base articulated systems at different poses. This tool can provide useful information for controller synthesis and assessment of the mechanical design of a system.

REFERENCES

- [1] M. Vukobratović and B. Borovac, “Zero-Moment Point—Thirty five years of its life,” *Int. J. Humanoid Rob.*, vol. 01, no. 01, pp. 157–173, 3 2004.
- [2] A. Hof, M. Gazendam, and W. Sinke, “The condition for dynamic stability,” *J. Biomech.*, vol. 38, no. 1, pp. 1–8, 1 2005.
- [3] T. Koolen, T. De Boer, J. Rebula, A. Goswami, and J. Pratt, “Capturability-based analysis and control of legged locomotion, Part 1: Theory and application to three simple gait models,” *Int. J. Rob. Res.*, vol. 31, no. 9, pp. 1094–1113, 8 2012.
- [4] J. Engelsberger, C. Ott, and A. Albu-Schäffer, “Three-Dimensional Bipedal Walking Control Based on Divergent Component of Motion,” *IEEE Trans. Rob.*, vol. 31, no. 2, pp. 355–368, 4 2015.
- [5] H. Dai and R. Tedrake, “Planning robust walking motion on uneven terrain via convex optimization,” in *IEEE-RAS Int. Conf. Humanoid Robots*, 2016, pp. 579–586.
- [6] H. Hirukawa, S. Hattori, K. Harada, S. Kajita, K. Kaneko, F. Kanehiro, K. Fujiwara, and M. Morisawa, “A universal stability criterion of the foot contact of legged robots - Adios ZMP,” in *Proc. IEEE Int. Conf. on Robotics and Automation*, 2006, pp. 1976–1983.
- [7] Y. Gu, B. Yao, and C. G. Lee, “Feasible center of mass dynamic manipulability of humanoid robots,” in *Proc. IEEE Int. Conf. on Robotics and Automation*, 2015, pp. 5082–5087.
- [8] R. Orsolino, M. Focchi, C. Mastalli, H. Dai, D. G. Caldwell, and C. Semini, “Application of wrench-based feasibility analysis to the online trajectory optimization of legged robots,” *IEEE Robot. Autom. Lett.*, vol. 3, no. 4, pp. 3363–3370, 2018.
- [9] J. Hwangbo, J. Lee, and M. Hutter, “Per-contact iteration method for solving contact dynamics,” *IEEE Robot. Autom. Lett.*, vol. 3, no. 2, pp. 895–902, 2018.
- [10] V. Delos and D. Teissandier, “Minkowski Sum of Polytopes Defined by Their Vertices,” *J. Appl. Math. and Phys.*, vol. 03, no. 01, pp. 62–67, 12 2015.
- [11] K. Fukuda and A. Prodon, “Double description method revisited,” in *Franco-Japanese and Franco-Chinese Conf. on Combinatorics and Computer Science*. Springer, 1995, pp. 91–111.
- [12] M. J. (2021) Analyze N-dimensional Convex Polyhedra. MATLAB Central File Exchange. [Online]. Available: <https://www.mathworks.com/matlabcentral/fileexchange/30892-analyze-n-dimensional-convex-polyhedra>
- [13] D. A. Winter, *Biomechanics and Motor Control of Human Movement: Fourth Edition*. Hoboken, N.J. :: Wiley., 2009, vol. 2nd.
- [14] C. Meijneke, G. Van Oort, V. Sluiter, E. Van Asseldonk, N. L. Tagliamonte, F. Tamburella, I. Pisotta, M. Masciullo, M. Arquilla, M. Molinari, A. R. Wu, F. Dzeladini, A. J. Ijspeert, and H. Van Der Kooij, “Symbitron Exoskeleton: Design, Control, and Evaluation of a Modular Exoskeleton for Incomplete and Complete Spinal Cord Injured Individuals,” *IEEE Trans. Neural Syst. Rehab. Eng.*, vol. 29, pp. 330–339, 2021.

APPENDIX I

PHYSICAL INCONSISTENCY OF THE NON-CAUSAL AWP COMPUTATION

The algorithm in [8] separates components of (1) into the ones that influence floating base dynamics (\square_f) and

the dynamics of the rest of the system/joints (\square_j). The manipulation is based on the fact that the floating base is not actuated, so the actuation forces u do not have an immediate influence on the floating base dynamics:

$$\begin{bmatrix} M_{ff} & M_{fj} \\ M_{jf} & M_{jj} \end{bmatrix} \begin{bmatrix} \dot{v}_f \\ \dot{v}_j \end{bmatrix} + \begin{bmatrix} h_f \\ h_j \end{bmatrix} = \begin{bmatrix} 0_{6 \times n_a} \\ \mathbb{I}_{n_a} \end{bmatrix} u + \begin{bmatrix} J_f^T \\ J_j^T \end{bmatrix} f \quad (21)$$

Therefore, the dynamics described by (1) *seem* to be decoupled, and, in principle the following operation can be used to solve for the contact forces:

$$f = (J_j^T)^+ ([M_{jf} \ M_{jj}] \dot{v} + h_j - u) \quad (22)$$

If we evaluate this equation for a given combination of torque limits we should be able to obtain the corresponding contact forces. However, to solve this equation both u and \dot{v} are needed. A given actuation input u and generalized acceleration of the form

$$\dot{v} = \dot{v}_s + \ker([M_{jf} \ M_{jj}]) \lambda$$

give the same contact force for any λ . For a chosen input acceleration \dot{v}_s and any null-space acceleration $\beta(\lambda) = \ker([M_{jf} \ M_{jj}]) \lambda$, (22) is satisfied, because $\beta(\lambda)$ does not have any effect in the resulting ground reaction force.

However, the floating base dynamics also need to hold, so we can actually find the null-space component of the acceleration in (22) that makes the dynamics consistent:

$$\begin{aligned} [M_{ff} \ M_{fj}] (\dot{v}_s + \beta(\lambda)) + h_f &= J_f^T f \\ \beta(f) &= [M_f \ M_{fj}]^+ (J_f^T f - h_f) - \dot{v}_s \end{aligned} \quad (23)$$

As f depends on \dot{v}_s and u (through (22)), the resulting generalized acceleration \dot{v} is indeed dependent on u and might differ from the provided input acceleration \dot{v}_s to satisfy the EoM:

$$\dot{v} = \dot{v}_s + \beta(\dot{v}_s, u) = \gamma(\dot{v}_s, u)$$

If we only consider *reactive* external forces, which is the case with contact, it is not possible that for a given u , two different \dot{v} are ‘achievable’. Thus, for the method from [8] to be physically consistent the \dot{v} resulting from a certain u and two different input accelerations \dot{v}_1 and \dot{v}_2 must be the same:

$$\gamma(\dot{v}_1, u) = \gamma(\dot{v}_2, u)$$

After some manipulation we obtain the following condition:

$$C(\dot{v}_1 - \dot{v}_2) = 0_{n_{DoF} \times 1}$$

with

$$C = [M_{ff} \ M_{fj}]^+ J_f^T (J_j^T)^+ [M_{jf} \ M_{jj}]$$

For this condition to always hold we need that $C = 0_{n_{DoF}}$ which is not true for all the configurations of an articulated system. Thus, decoupling the dynamics of each leg and providing an input acceleration to compute the force result in physically inconsistent forces.